Published in final edited form as:

J Orthop Res. 2015 November ; 33(11): 1693–1703. doi:10.1002/jor.22928.

Improved Biomechanical and Biological Outcomes in the MRL/MpJ Murine Strain Following a Full-Length Patellar Tendon Injury

Andrea L. Lalley[1], **Nathaniel A. Dyment**[2], **Namdar Kazemi**[3], **Keith Kenter**[3], **Cynthia Gooch**[1], **David W. Rowe**[2], **David L. Butler**[1], and **Jason T. Shearn**[1]

[1]Biomedical Engineering Program, College of Engineering and Applied Science, University of Cincinnati, Cincinnati, Ohio

[2]Department of Reconstructive Sciences, College of Dental Medicine, University of Connecticut Health Center, Farmington, Connecticut

[3]Department of Orthopaedic Surgery, College of Medicine, University of Cincinnati, Cincinnati, Ohio

Abstract

Musculoskeletal injuries greatly affect the U.S. population and current clinical approaches fail to restore long-term native tissue structure and function. Tissue engineering is a strategy advocated to improve tendon healing; however, the field still needs to establish biological benchmarks for assessing the effectiveness of tissue-engineered structures. Investigating superior healing models, such as the MRL/MpJ, offers the opportunity to first characterize successful healing and then apply experimental findings to tissue-engineered therapies. This study seeks to evaluate the MRL/MpJ's healing response following a central patellar tendon injury compared to wildtype. Gene expression and histology were assessed at 3, 7, and 14 days following injury and mechanical properties were measured at 2, 5, and 8 weeks. Native patellar tendon biological and mechanical properties were not different between strains. Following injury, the MRL/MpJ displayed increased mechanical properties between 5 and 8 weeks; however, early tenogenic expression patterns were not different between the strains. Furthermore, expression of the cyclin-dependent kinase inhibitor, p21, was not different between strains, suggesting an alternative mechanism may be driving the healing response. Future studies will investigate collagen structure and alignment of the repair tissue and characterize the complete healing transcriptome to identify mechanisms driving the MRL/MpJ response.

Correspondence to: Jason T. Shearn (T: 513-556-4171; F: 513-556-4162; shearnj@ucmail.uc.edu).

Conflict of interest: None.

AUTHORS' CONTRIBUTIONS

Experiment conception and design completed by AL, ND, NK, KK, CG, DB, JS. Experiment execution completed by AL, ND, NK, CG. Data analysis and interpretation completed by AL, ND, NK, KK, CG, DB, JS. Experimental materials contributed by ND, KK, DR, DB, JS. The paper was written and edited by AL, ND, NK, KK, CG, DR, DB, JS.

SUPPORTING INFORMATION

Additional supporting information may be found in the online version of this article.

Keywords

tendon; tendon healing; MRL/MpJ; p21

INTRODUCTION

Musculoskeletal injuries, particularly to tendons and ligaments, are frequent and present a large burden on the U.S. economy.[1,2] While current treatment strategies often accelerate a patient's return to pre-injury activity levels through direct repair or replacement of the damaged tissue, long-term outcomes lead to increased rates of re-injury or the development of chronic conditions, such as osteoarthritis.[3,4] New therapeutic strategies are needed to improve the shortcomings associated with current clinical practices.

Tissue engineering has proved to be a promising approach; however, previous attempts have focused on meeting the mechanical demands of the tissue as established by the functional tissue engineering paradigm.[5] Previous tissue engineering studies in our laboratory using autologous mesenchymal progenitor cells (MPCs) seeded in a collagen scaffold and implanted into a rabbit central patellar tendon (PT) defect showed moderate success. The tendon repair tissue matched normal PT up to 32% of normal failure force, 50% beyond peak in vivo forces measured for activities of daily living, by 12 weeks post injury; however, serial fiber failures initiated beyond 32% of normal failure force.[6] Exposing this repair tissue to more strenuous activity levels would presumably lead to ultimate failure. While these results show promise, the tissue engineering field needs to establish biological success criteria to benchmark future therapies.[7] Understanding adult, scar-free healing may provide valuable information that can be used to stimulate natural healing processes to achieve successful tissue formation following injury.

Tissue regeneration is limited in the mammalian kingdom; however, the Murphy Roths Large (MRL/ MpJ) murine strain has been identified as a potential model of successful mammalian healing following injury. Originally created to investigate systemic lupus erythematosis, this mouse was found to repair identifying ear hole punches via the development of a blastema and subsequent reformation of sebaceous glands, hair follicles, and aligned collagen.[8] Further studies have shown regenerative-like healing in other tissues including cornea,[9] heart,[10] spinal cord,[11,12] and articular cartilage,[13,14] although with varying degrees of healing. In some cases, the MRL/MpJ healing proved no better than wild type,[15,16] suggesting the response may be dependent on the type or severity of the induced injury. Currently, the field is divided on what is driving the MRL/MpJ healing phenotype. Through genetic analysis, mutations were found to be distributed over 20 different loci on 7 chromosomes,[17] suggesting multiple factors may be involved in the phenotype making it difficult to isolate one particular pathway or target of interest for study.

Several investigators suggest the phenotype may be a result of a mutation causing decreased expression of the cyclin-dependent kinase inhibitor, p21.[18–20] This molecule is a downstream effector of the tumor suppresser, p53, acting at the G1 checkpoint to prevent cell cycle progression to S phase in the event of DNA damage.[19] Studies investigating the MRL/MpJ healing process have shown p21 to be expressed below normal levels both in cells

derived from non-injured tissue and in cells participating throughout the healing process[18–20]; however, it remains unclear if this single mechanism is truly driving the MRL/MpJ healing process.[21]

Given the poor natural healing outcomes following tendon injury, investigating the MRL/MpJ healing response offers the opportunity to characterize a superior form of tendon healing. Driving tissue-engineered repairs down a regenerative-like pathway, as opposed to a natural healing pathway, may be key in restoring native tissue structure and function. Thus, the objective of this study was to evaluate the healing potential of the MRL/MpJ murine strain in response to a full-length, full-thickness central PT injury compared to C57BL/6 controls based on biomechanical, biological, and morphological outcome measures. We hypothesized the MRL/MpJ would exhibit (i) improved biomechanical outcomes, (ii) increased expression of tendon-related genes, and (iii) decreased expression of p21 compared to the C57BL/6 strain.

METHODS

Experimental Design

PT physical dimensions, structural and material properties, tissue morphology, and gene expression levels were assessed following a full-length, full-thickness central PT injury in 20-week old male C57BL/6 mice (20.6 ± 0.3 weeks; mean ± SD) and MRL/MpJ mice (20.4 ± 0.5 weeks; mean ± SD). Breeding pairs for the C57BL/6 (stock number: 000664) and MRL/MpJ (stock number: 000486) strains were obtained from The Jackson Laboratory (Bar Harbor, ME) and bred in-house. Following injury, natural tendon healing based on biomechanical outcomes at 2, 5, and 8 weeks (n = 8–14 per time point), histology at 3, 7, and 14 days (n = 2 per time point), and gene expression at 3, 7, and 14 days (n = 3 per time point) was compared between the MRL/MpJ strain and C57BL/6 control strain (Table 1). Inter-animal comparisons were made to respective native, uninjured PTs from age-matched MRL/MpJ and C57BL/6 mice.

Surgical Procedure

All protocols and procedures were reviewed and approved by the University of Cincinnati's Institutional Animal Care and Use Committee. The surgical procedure has been previously described.[22] Briefly, animals were anesthetized through inhalation of 3% isoflurane and the hindlimbs were prepared using 70% alcohol and betadine washes. The PT was exposed and medial and lateral longitudinal incisions were created on either side of the PT. Jeweler's forceps were slipped beneath the tendon to isolate it from surrounding tissues and tensioned. An incision was made with a scalpel to create the lateral edge of the tendon defect and a modified Jeweler's forceps was then slipped through this incision and pushed up through the tendon to create the medial edge. The central-third of the PT was then removed with a scalpel at both the patella and tibial insertions. A modified jigsaw blade was used to disrupt the tibial insertion. In the contralateral limb, a sham procedure was completed in which the jeweler's forceps were slipped under the tendon; however, no central defect was created. Incisions were closed using 5–0 prolene suture (Ethicon, Somerville, NJ) and animals were

allowed unrestricted cage activity. Mice were euthanized by carbon dioxide asphyxiation and cervical dislocation.

Biomechanical Testing

Animals were frozen at −20°C until the day of testing. Prior to testing, limbs were thawed, skin and muscle was removed, and the knee joint was flexed to 45°. In the defect limb, the struts were removed leaving the patella–PT repair tissue–tibia unit. In the flexed position, the PT repair length and width were optically measured by taking a digital image with a ruler in plane. The sham limb was cut down to a similar width. The tibia portion of the specimen was cemented in a grip with polymethylacrylate (Dentspyly International, York, PA) and secured with a staple to prevent axial slipping. The specimen was loaded into a materials testing system (100R; TestResources, Shakopee, MN) and lowered to fix the patella into the bottom grip. A preload of 0.02 N was applied and the PT thickness was measured by taking a digital image with a ruler in plane with the PT. All measurements (PT length, width, and thickness) were measured using Fiji (image analysis software based on ImageJ; version 1.47). The tissue was tested in a 37°C PBS bath by preconditioning for 25 cycles between 0% and 1% strain and then failed in uniaxial tension at 0.1% of total tendon length/second.[23] The applied load and grip-to-grip displacement were recorded throughout the testing period. Ultimate load (UL), failure displacement, stress, and strain were recorded during the testing period. Linear stiffness (LS) and modulus were calculated from the linear portion of the load–displacement and stress–strain curves, respectively.

Histological and Immunohistochemical Sample Preparation

Twenty-four hours prior to sacrifice, animals assigned to histology/IHC were administered an intraperitoneal injection of EdU (5-ethynyl-2′-deoxyuridine, Invitrogen, Grand Island, NY) at a concentration of 3 μg/g body weight to assess cellular proliferation occurring at 3, 7, and 14 days following surgery. After sacrifice, each limb was fixed in 4% paraformaldehyde (Fisher Scientific, Pittsburgh, PA) for 24 h. Samples were decalcified with 0.5M EDTA/PBS for 7 days at 4°C and then embedded in O.C.T. compound (Andwin Scientific Tissue-Tek ™, Schaumburg, IL) for frozen sectioning. Six sets of equally-spaced transverse 8 μm sections (approximately 0.5 mm apart) were cut using a Leica CM3050S cryostat (Leica, Wetzlar, Germany) with cryofilm (Cryofilm Type 2C, Section-lab, Hiroshima, Japan). Sections were affixed to glass slides and allowed to dry for 48 h at room temperature.

Histology and Immunohistochemistry

Sections were incubated in blocking solution (0.1% Triton X-100 and 1% BSA in PBS) for 1 h and then incubated for either one hour at room temperature or overnight at 4°C with a combination of the following primary antibodies: rabbit anti-collagen type VI (1:50, sc-20649, Santa Cruz Biotechnology, Dallas, TX), goat anti-collagen type I (1:100, AB758, EMD Millipore, Billerica, MA), rabbit anti-tenascin-C (1:500, ab6346, Abcam), or rat anti-F4/80 (1:100, 123102, BioLegend, San Diego, CA). Following incubation with primary antibody, sections were washed in PBS and then incubated in appropriate secondary antibody (Alexa Fluor IgG; Invitrogen) for 1 h at room temperature. Goat anti-rabbit (488 nm) was used for the collagen type VI antibody, goat anti-rat (647 nm) was used for the

tenascin-C primary antibody, and donkey anti-goat (594 nm) was used for the collagen type I primary antibody. Following incubation, sections were washed and stained with DAPI to visualize cell nuclei and photographed using an Axio Scan.Z1 microscope (Carl Zeiss Microscopy, Thornwood, NY) at 10× magnification. Following imaging, sections were washed, stained for EdU (Click-iT® EdU Alexa Fluor® 647 Imaging Kit, C10340, Life Technologies), and reimaged to capture actively proliferating cells.

Quantification of Proliferating Cells

Grayscale images for EdU and DAPI were equally thresholded for all groups and converted to binary images. The DAPI image was overlaid on to the EdU image to identify cells that were EdU positive. Total cell number (all DAPI positive cells) and EdU positive nuclei (cells positive for both DAPI and EdU) were then counted by thresholding upper and lower size bounds using FIJI particle counter.

Quantitative Real-Time PCR (qPCR)

Following sacrifice, the defect midsubstance was isolated and 3 tendons were pooled per sample. Native tendon midsubtance samples served as the control. Tissue samples were placed in RNAlater® (Invitrogen) and stored at −20°C. The RNAeasy® Mini Kit (74104; Qiagen, Venlo, Limburg) was used to isolate RNA. The tissue was ground using a pestle, vortexed, and centrifuged. The supernatant was passed through a spin column and an on-column DNase digestion was performed following the RNase-Free DNase Set protocol (79254; Qiagen). The RNA was eluted and quantified using a NanoDrop ND-1000 Spectrophotometer (NC9904842, Nano-Drop Technologies, Inc, Wilmington, DE). RNA was converted to cDNA using the High Capacity RNA-to-cDNA kit (4387406; Applied Biosystems, Grand Island, NY). Real-time qPCR reactions were run using Taqman® Gene Expression Fast Mastermix and Taqman® Gene Expression Assays (Table 2) (4364103; Applied Biosystems). Delta C_T values were computed and normalized to 18S expression within each sample. Delta delta C_T values were computed by normalizing to respective native tendon.

Statistical Analysis

All data sets were verified to be homoscedastic and normally distributed prior to statistical testing. Native MRL/MpJ and C57BL/6 tendon dimensions, mechanical properties, and gene expression values were compared using independent Student's *t*-test. Native, defect, and sham mechanical properties were evaluated via 3-way ANOVA with time post-surgery, strain, and treatment set as fixed factors with Fisher's Least Significant Difference (LSD) and a bonferonni correction for multiple comparisons. A total of five comparisons were made with a significance level of $p = 0.01$. Gene expression was evaluated via Kruskal–Wallis with time post-surgery and murine strain set as fixed factors followed by Mann-Whitney U with bonferroni correction for post hoc testing. Cellular proliferation was assessed using independent Student's t-test between strains at each time point. The IBM SPSS Statistics 2.1.0 software (Chicago, IL) was used to perform all statistical testing.

RESULTS

Native Patellar Tendon Properties of C57BL/6 versus MRL/ MpJ

The MRL/MpJ had significantly larger intact PT width (1.22 ± 0.26 mm vs. 1.00 ± 0.11 mm, $p = 0.009$) compared to the C57BL/6; however, the central MRL/MpJ and C57BL/6 PT widths (0.55 ± 0.05 mm vs. 0.58 ± 0.03 mm, $p = 0.052$), lengths (3.07 ± 0.11 mm vs. 2.95 ± 0.11 mm, $p = 0.013$), thicknesses (0.45 ± 0.03 mm vs. 0.47 ± 0.06 mm, $p = 0.364$), and cross-sectional areas ($p = 0.065$) were not different were not different between the two strains.

No significant differences were noted in the mechanical properties. MRL/MpJ and control tendons showed similar UL ($p = 0.781$), LS ($p = 0.582$), maximum stress ($p = 0.409$), and elastic modulus ($p = 0.052$) (Fig. 1 and Table 3). We also found there were minimal differences among expression levels of the genes of interest (Table 4). The MRL/MpJ tissue showed slightly elevated collagen type I expression compared to C57BL/6 ($p = 0.048$) with no other tenogenic markers showing significant expression differences ($p > 0.01$). p21 expression between the two strains was not different ($p = 0.422$).

The MRL/MpJ Healing Response Produces Improved Structural and Material Properties Following Tendon Injury by 8 Weeks

Murine strain, time post surgery, and surgical treatment each significantly affected cross-sectional area and structural properties. UL and LS in both the C57BL/6 and MRL/MpJ strains were significantly reduced compared to respective native values at 2- and 5-week values ($p < 0.01$). However, the MRL/MpJ tendons displayed increased LS compared to C57BL/6 at the 2-week time point, although not statistically significant (6.50 ± 1.43 N vs. 4.50 ± 0.66 N, $p = 0.042$, $p < 0.01$). By 8 weeks, the MRL/MpJ achieved 81% of native UL (3.48 ± 0.92 N vs. 4.31 ± 1.53 N, $p = 0.078$) and 77% of native LS (7.21 ± 1.00 N/mm vs. 9.31 ± 1.99 N/mm, $p = 0.001$) while the C57BL/6 achieved only 41% of native UL (1.82 ± 0.66N vs. 4.44 ± 0.75 N, $p < 0.001$) and 59% of native LS (5.72 ± 0.85 N vs. 9.76 ± 1.30 N, $p < 0.001$). Furthermore, the MRL/MpJ showed increases in UL and LS parameters between 5 and 8 weeks and were significantly greater than C57BL/6 UL by 8 weeks (3.48 ± 0.92 N vs. 1.82 ± 0.66 N; $p < 0.01$). The C57BL/6 structural properties plateaued, failing to improve beyond the 2-week time point (Table 3, Fig. 2a and b, Fig. 3a and b).

Time post surgery and surgical treatment significantly affected ultimate stress and modulus in both strains ($p < 0.01$; Table 3, Fig. 2a and b). Compared to native, both the C57BL/6 and MRL/MpJ strains showed reduced values for ultimate stress and modulus at 2, 5, and 8 weeks ($p < 0.01$; Table 3, Fig. 2a and b, Fig. 3c and d). While the C57BL/6 reached a plateau following the 2-week time point ($p > 0.01$), the MRL/ MpJ showed improved ultimate stress and modulus between 5 and 8 weeks, but were still significantly less than native ($p < 0.01$).

Tenogenic Expression Profiles are Not Different between MRL/MpJ and C57BL/6 at 3, 7, and 14 Days Post Surgery

Although murine strain did not affect gene expression ($p > 0.01$), time post surgery did significantly influence expression levels ($p < 0.01$). We found no statistical differences between strains for the genes of interest at any time point (Table 4).

Collagens—For the C57BL/6 strain, Col1a1 expression peaked at day 7 but returned to normal levels by day 14. Col3a1 expression levels were elevated at 3, 7, and 14 days following injury, peaking at day 7. The MRL/MpJ showed a similar trend for collagen expression levels; however, Col1a1 expression remained elevated at day 14.

Proteoglycans and Glycoproteins—At day 3, Dcn, Fmod, and Tnmd expression were decreased in both strains compared to their respective native controls. By day 7, Dcn, Fmod, and Tnmd expression returned to normal levels in the MRL/MpJ. In the C57BL/6, Dcn expression was no different than normal at day 7, but was decreased at day 14. Fmod expression was decreased at day 7, but returned to normal levels by day 14, while Tnmd expression returned to normal levels at day 7. Tenascin-C expression was elevated in the MRL/MpJ at day ($p < 0.01$), and did not show any differences for C57BL/6 with respect to time.

Transcription Factors—Egr1, Mkx, and Scx expression were not altered following injury in either strain ($p > 0.01$). Mkx and Scx expression levels showed similar temporal trends, showing decreased expression at day 3, but a return to normal levels by day 7.

MRL/MpJ Repair Tissue Shows Increased Cellular Proliferation Compared to C57BL/6 but is not a Result of a p21 Deficiency

At 3 days post injury, there were no differences in proliferation between the two strains ($p = 0.41$). At 7 and 14 days following injury, the MRL/MpJ showed significantly increased cellular proliferation ($p = 0.002$ and $p = 0.037$, respectively) compared to the C57BL6, reaching 14.1% and 4.8%, respectively (Fig. 4). We found no difference in p21 expression between the two strains at post-surgical time points (Fig. 5). Both strains displayed increased expression of p21 at 3 days following injury ($p < 0.05$); however, expression levels were not different than native values at 7 or 14 days for either strain (Table 4).

The MRL/MpJ Shows a Reduced Immunological Response Following Injury

We evaluated macrophage infiltration following injury by staining for F4/80, a membrane protein found on macrophages and microglial cells. Native C57BL/6 and MRL/MpJ tissues showed no differences in expression (Fig. 6a and b); however, compared to the C57BL/6 at corresponding time points post injury, the MRL/MpJ macrophage concentration is quantitatively decreased at 3, 7, and 14 days (Fig. 6). Although, both strains show increased macrophage presence following injury, expression was more pronounced in the C57BL/6, especially at the day 7 timepoint (Fig. 6e and f).

DISCUSSION

The objective of this study was to evaluate the utility of the MRL/MpJ as a murine model of improved healing following a full-length, full-thickness central PT injury based on mechanical, histological, and biological response measures. We initially compared the native PT tissues for both the MRL/MpJ and C57BL/6 and found no differences with respect to mechanical properties or gene expression values for tendon-related markers or markers involved in the p21 pathway. This was of particular interest because previous studies have suggested abnormal regulation of p21 is a major contributor to the healing phenotype.[18,24] Following full-length, full-thickness PT injury, the MRL/MpJ displayed enhanced cellular proliferation at 7 and 14 days. Further, our findings suggest we cannot rule out the possibility that there were no differences in expression of tendon-related genes or p21 expression between the strains. While the mechanical outcomes showed little difference between the two strains at 2 and 5 weeks, the MRL/MpJ showed improvements to structural and material properties between 5 and 8 weeks post injury, reaching 81% and 77% of native US and LS, respectively.

Our results suggest that the initial response to tendon injury in each of these strains is similar with respect to overall healing progression and expression of tenogenic markers measured at 3, 7, and 14 days post injury (Supp. Fig. 1). The differences in the healing processes did not manifest until later time points when it was observed that the MRL/MpJ showed improvements in structural and material properties between 5 and 8 weeks while the C57BL/6 plateaued at 2 weeks. This could suggest the MRL/MpJ healing process extends beyond the 2-week time point, with continued matrix production and remodeling occurring. Studies have shown that the accumulation of tendon mechanical properties during early post-natal development takes several months, resulting from increases in collagen content, mean fibril diameter, and proteoglycan and glycoprotein concentration.[25–27] The MRL/MpJ healing process could be progressing in much the same way, continuing to show increases in mechanical strength and tissue integrity for several weeks following injury.

The differences between strains with respect to cellular proliferation and immune cell infiltration at early time points, coupled with improved mechanical outcomes at later time points, indicate an alternative mechanism is likely regulating the MRL/MpJ healing process. Questions remain as to the pathways that drive the MRL/ MpJ response. Answering these questions has been difficult because observed healing outcomes have varied widely in the MRL/MpJ following injury to a number of tissue systems.[9,13,15,24,28] A mutation causing decreased expression of the cyclin-dependent kinase inhibitor, p21, has been proposed as a potential driver of the healing phenotype causing increased cellular proliferation despite DNA damage.[18,24] In this study, we observed increased cellular proliferation in the MRL/MpJ compared to wildtype at 7 and 14 days; however, p21 expression was increased compared to native expression in the MRL/MpJ at these time points. Based on our results, we could not rule out the possibility that MRL/ MpJ p21 expression was not different when compared to p21 expression in the C57BL/6 at any time point. This finding would suggest that the regenerative capacity may lie in an alternative pathway unrelated to the p21 mechanism or that mechanisms regulating the healing phenotype may differ depending on the type of injury and/or injury location.[29,30]

Findings from studies investigating the MRL/MpJ mouse point to decreased inflammatory and immunological responses following injury that may be driving the healing phenotype9, 21, 31, 32. We compared F4/80 expression, a membrane protein that demarcates macrophages and microglial cells, in the healing tissue between the two strains and found the MRL/MpJ showed decreased expression, suggesting the immune response may be reduced compared to the wildtype response. Based on previous reports showing improved skin repair in neutrophil-depleted mice, Ueno et al. investigated corneal healing in both the MRL/MpJ strain and neutrophil-depleted mice9. They postulated infiltrating neutrophils might slow the re-epithelialization process, leading to poor healing outcomes in the wildtype animal. Both the MRL/MpJ and neutrophil-depleted mice showed enhanced re-epithelialization and healing outcomes compared to wildtype; however, the MRL/MpJ's response was accelerated compared to the neutrophil-depleted mice, suggesting the phenotype is not solely a result of a decreased immunological response9. The MRL/MpJ healing phenotype may result from a retention of embryonic-like features characteristic of normal development.[33] Naviaux et al. found the MRL/MpJ strain expressed Nanog in uninjured heart tissue along with a 10-fold increase following a cryoinjury with negligible expression measured in the wildtype. Similar expression patterns were observed for Islet-1 and Sox2, two other pluripotential markers. We measured expression of scleraxis, mohawk homeobox, and early growth response 1, three transcription factors known to be highly involved in tendon development and maturation; however, we found no differences in expression between the two strains. We did not; however, measure expression of markers that could be upstream of these transcription factors during the developmental stages. Future work will investigate the similarities between normal tendon development and regenerative models to develop the metrics for assessing tissue engineering and repair strategies.

Previous work has shown the MRL/MpJ healing response varies significantly depending on the injury modality and tissue type.[8,15,16,24] The original work identifying the MRL/MpJ as a potential model to study mammalian regeneration following an ear-hole punch found the skin tissue that formed was characterized by the reformation of sebaceous glands, hair follicles, well-aligned collagen, and cartilage formation by 12 weeks.[8] Based on these findings, the authors claimed the response was regenerative in nature; however, Colwell et al. reported the MRL/MpJ showed similar levels of fibrosis compared to the C57BL/6 at 28 days post-injury following dorsal cutaneous skin wounds.[16] Ueno et al. investigated corneal healing following an alkali-burn injury and reported the MRL/MpJ exhibited accelerated re-epithelialization accompanied by decreased inflammation and fibrosis.[9] The authors suggest the MRL/ MpJ implements an alternative healing mechanism compared to wildtype producing superior outcomes, although do not go as far to say the response is regenerative in nature.[9] Clearly, differences in tissue type, injury modality, and experimental design and execution can all contribute to variable outcomes.

It is difficult to draw direct comparisons in the healing capabilities of the MRL/MpJ in various tissue types due to the differences in the functional demands of each tissue; however, articular cartilage has been investigated, providing one example of musculoskeletal tissue healing in this strain. Fitzgerald et al. created both full-thickness lesions in the trochlear groove in the MRL/MpJ and wildtype and found that by 12 weeks, the MRL/MpJ showed elevated levels of collagen types II and VI along with increased expression of proteoglycans,

significantly greater than wild-type.[13] Similar to the study by Fitzgerald, findings from our study suggest the MRL/MpJ does not repair excisional tendon injuries via a purely scar-free mechanism, rather this strain shows a similar healing progression as wildtype initially (Supp. Fig. 1), but may exhibit a prolonged healing response leading to the superior properties by 8 weeks post-injury.

This study is not without limitations. (i) We only evaluated gene expression at early post-surgical time points. Future work should investigate gene expression at 5, 8, and 10 weeks to better understand the molecular events that are contributing to the mechanical results observed at these later time points. (ii) The PT injury that we utilize is not clinically relevant. Tendon and ligament injuries occurring in the patient population are often accompanied by an underlying chronic condition, termed tendinopathy.[34,35] Our murine model fails to incorporate aspects of tendinopathy making direct comparisons to the clinical condition difficult. While this is a limitation, investigating tendon injuries in a well-controlled environment minimizes potential confounding variables. Future work should investigate developing a model system that faithfully recapitulates aspects of tendinopathy. Findings from this study could be applied to this future model. (iii) The physical dimensions of the PT were obtained by optical measurement via digital image. Previous work has shown the cross-sectional area changes along the length of the PT and assuming a uniform cross-sectional area may lead to an overestimation or underestimation of material properties. Future studies utilizing mechanical testing as a response measure should include a more precise method of obtaining physical dimensions, such as a laser reflectance system or quantitative ultrasound.[36,37] (iv) Finally, the results reported for gene expression analysis and histological assessment are based on small sample sizes (N = 3 and N = 2, respectively). Future work should include increasing the sample sizes for both response measures to further substantiate the findings presented here.

While it remains unclear if the MRL/MpJ is a model of true regeneration, findings from this study support further characterization of this model to identify novel pathways to target with future tissue-engineered therapies. This strategy will also allow for defining biological success criteria to benchmark tissue-engineered constructs and repairs.

Supplementary Material

Refer to Web version on PubMed Central for supplementary material.

Acknowledgments

Grant sponsor: National Institutes of Health grant R01; Grant number: AR056943.

This work was supported by the National Institutes of Health grant R01 AR056943. The authors declare they have no actual or competing financial interests. We thank Dr. Andrew Breidenbach and Steve Gilday for surgical and technical assistance.

References

1. Praemer, A.; Furner, S.; Rice, DP. Musculoskeletal Conditions in the United States. 2. Rosemont, Illinois: American Acadmey of Orthopaedic Surgeons; 1999.

2. United States Bone and Joint Initiative. The Burden of Musculoskeletal Diseases n the United States. Rosemont, IL: American Academy of Orthpaedic Surgeons; 2008. American Academy of Orthopedic Surgeons

3. Gifstad T, Sole A, Strand T, Uppheim G, et al. Long-term follow-up of patellar tendon grafts or hamstring tendon grafts in endoscopic ACL reconstructions. Knee Surg Sports Traumatol Arthrosc. 2013; 21:576–583. [PubMed: 22407182]

4. Keays SL, Bullock-Saxton JE, Keays AC, et al. A 6-year follow-up of the effect of graft site on strength, stability, range of motion, function, and joint degeneration after anterior cruciate ligament reconstruction: patellar tendon versus semitendinosus and Gracilis tendon graft. Am J Sports Med. 2007; 35:729–739. [PubMed: 17322130]

5. Butler DL, Goldstein SA, Guilak F. Functional tissue engineering: the role of biomechanics. J Biomech Eng. 2000; 122:570–575. [PubMed: 11192376]

6. Butler DL, Juncosa-Melvin N, Boivin GP, et al. Functional tissue engineering for tendon repair: a multidisciplinary strategy using mesenchymal stem cells, bioscaffolds, and mechanical stimulation. J Orthop Res. 2008; 26:1–9. [PubMed: 17676628]

7. Breidenbach AP, Gilday SD, Lalley AL, et al. Functional tissue engineering of tendon: Establishing biological success criteria for improving tendon repair. J Biomech. 2013

8. Clark LD, Clark RK, Heber-Katz E. A new murine model for mammalian wound repair and regeneration. Clin Immunol Immunopathol. 1998; 88:35–45. [PubMed: 9683548]

9. Ueno M, Lyons BL, Burzenski LM, et al. Accelerated wound healing of alkali-burned corneas in MRL mice is associated with a reduced inflammatory signature. Invest Ophthalmol Vis Sci. 2005; 46:4097–4106. [PubMed: 16249486]

10. Leferovich JM, Bedelbaeva K, Samulewicz S, et al. Heart regeneration in adult MRL mice. Proc Natl Acad Sci USA. 2001; 98:9830–9835. [PubMed: 11493713]

11. Donnelly DJ, Popovich PG. Inflammation and its role in neuroprotection, axonal regeneration and functional recovery after spinal cord injury. Exp Neurol. 2008; 209:378–388. [PubMed: 17662717]

12. Thuret S, Thallmair M, Horky LL, et al. Enhanced functional recovery in MRL/MpJ mice after spinal cord dorsal hemisection. PLoS One. 2012; 7:e30904. [PubMed: 22348029]

13. Fitzgerald J, Rich C, Burkhardt D, et al. Evidence for articular cartilage regeneration in MRL/MpJ mice. Osteoarthritis Cartilage. 2008; 16:1319–1326. [PubMed: 18455447]

14. Rai MF, Hashimoto S, Johnson EE, et al. Heritability of articular cartilage regeneration and its association with ear wound healing in mice. Arthritis Rheum. 2012; 64:2300–2310. [PubMed: 22275233]

15. Abdullah I, Lepore JJ, Epstein JA, et al. MRL mice fail to heal the heart in response to ischemia-reperfusion injury. Wound Repair Regen. 2005; 13:205–208. [PubMed: 15828946]

16. Colwell AS, Krummel TM, Kong W, Longaker MT, Lorenz HP. Skin wounds in the MRL/MPJ mouse heal with scar. Wound Repair Regen. 2006; 14:81–90. [PubMed: 16476076]

17. Masinde GL, Li X, Gu W, et al. Identification of wound healing/regeneration quantitative trait loci (QTL) at multiple time points that explain seventy percent of variance in (MRL/MpJ and SJL/J) mice F2 population. Genome Res. 2001; 11:2027–2033. [PubMed: 11731492]

18. Bedelbaeva K, Snyder A, Gourevitch D, et al. Lack of p21 expression links cell cycle control and appendage regeneration in mice. Proc Natl Acad Sci USA. 2010; 107:5845–5850. [PubMed: 20231440]

19. Arthur LM, Heber-Katz E. The role of p21 in regulating mammalian regeneration. Stem Cell Res Ther. 2011; 2:30. [PubMed: 21722344]

20. Arthur LM, Demarest RM, Clark L, et al. Epimorphic regeneration in mice is p53-independent. Cell Cycle. 2010; 9:3667–3673. [PubMed: 20855943]

21. Sereysky JB, Flatow EL, Andarawis-Puri N. Musculo-skeletal regeneration and its implications for the treatment of tendinopathy. Int J Exp Pathol. 2013; 94:293–303. [PubMed: 23772908]

22. Dyment NA, Kazemi N, Aschbacher-Smith LE, et al. The relationships among spatiotemporal collagen gene expression, histology, and biomechanics following full-length injury in the murine patellar tendon. J Orthop Res. 2012; 30:28–36. [PubMed: 21698662]

23. Robinson PS, Huang TF, Kazam E, et al. Influence of decorin and biglycan on mechanical properties of multiple tendons in knockout mice. J Biomech Eng. 2005; 127:181–185. [PubMed: 15868800]
24. Bedelbaeva K, Gourevitch D, Clark L, et al. The MRL mouse heart healing response shows donor dominance in allogeneic fetal liver chimeric mice. Cloning Stem Cells. 2004; 6:352–363. [PubMed: 15671663]
25. Ansorge HL, Adams S, Birk DE, et al. Mechanical, compositional, and structural properties of the post-natal mouse Achilles tendon. Ann Biomed Eng. 2011; 39:1904–1913. [PubMed: 21431455]
26. Ansorge HL, Hsu JE, Edelstein L, et al. Recapitulation of the Achilles tendon mechanical properties during neonatal development: a study of differential healing during two stages of development in a mouse model. J Orthop Res. 2012; 30:448–456. [PubMed: 22267191]
27. Ansorge HL, Adams S, Jawad AF, et al. Mechanical property changes during neonatal development and healing using a multiple regression model. J Biomech. 2012; 45:1288–1292. [PubMed: 22381737]
28. Tucker B, Klassen H, Yang L, et al. Elevated MMP Expression in the MRL Mouse Retina Creates a Permissive Environment for Retinal Regeneration. Invest Ophthalmol Vis Sci. 2008; 49:1686–1695. [PubMed: 18385092]
29. Beare AH, Metcalfe AD, Ferguson MW. Location of injury influences the mechanisms of both regeneration and repair within the MRL/MpJ mouse. J Anat. 2006; 209:547–559. [PubMed: 17005026]
30. Heydemann A. The super super-healing MRL mouse strain. Front Biol (Beijing). 2012; 7:522–538. [PubMed: 24163690]
31. Dovi JV, He LK, DiPietro LA. Accelerated wound closure in neutrophil-depleted mice. J Leukoc Biol. 2003; 73:448–455. [PubMed: 12660219]
32. Tolba RH, Schildberg FA, Decker D, et al. Mechanisms of improved wound healing in Murphy Roths Large (MRL) mice after skin transplantation. Wound Repair Regen. 2010; 18:662–670. [PubMed: 20946143]
33. Naviaux RK, Le TP, Bedelbaeva K, et al. Retained features of embryonic metabolism in the adult MRL mouse. Mol Genet Metab. 2009; 96:133–144. [PubMed: 19131261]
34. Millar NL, Hueber AJ, Reilly JH, et al. Inflammation is present in early human tendinopathy. Am J Sports Med. 2010; 38:2085–2091. [PubMed: 20595553]
35. Scott A, Docking S, Vicenzino B, et al. Sports and exercise-related tendinopathies: a review of selected topical issues by participants of the second International Scientific Tendinopathy Symposium (ISTS) Vancouver 2012. Br J Sports Med. 2013; 47:536–544. [PubMed: 23584762]
36. Moon DK, Abramowitch SD, Woo SL. The development and validation of a charge-coupled device laser reflectance system to measure the complex cross-sectional shape and area of soft tissues. J Biomech. 2006; 39:3071–3075. [PubMed: 16413929]
37. Pokhai GG, Oliver ML, Gordon KD. A new laser reflectance system capable of measuring changing cross-sectional area of soft tissues during tensile testing. J Biomech Eng. 2009; 131:094504. [PubMed: 19725701]

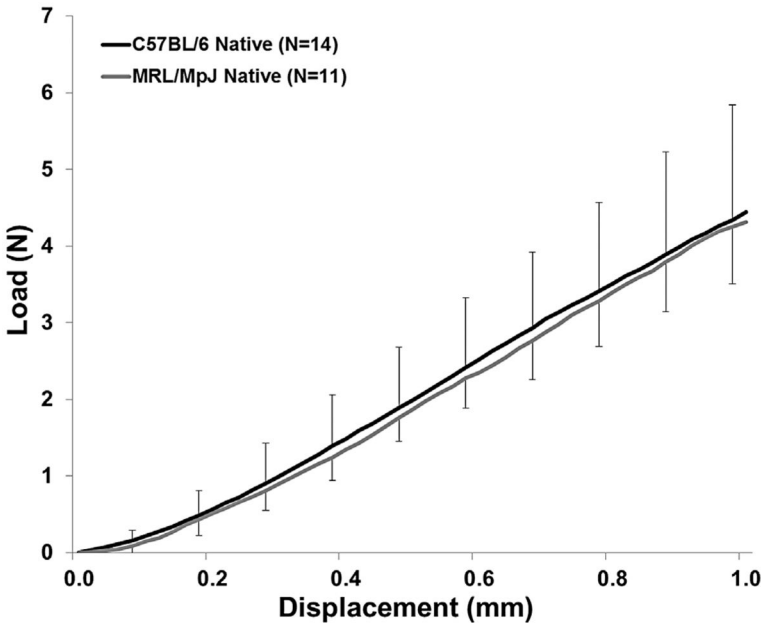

Figure 1.

Load-displacement failure curves for native 20-week old C57BL/6 and MRL/MpJ patellar tendon. There were no significant differences in structural properties between the two strains ($p > 0.05$). Error bars represent SD.

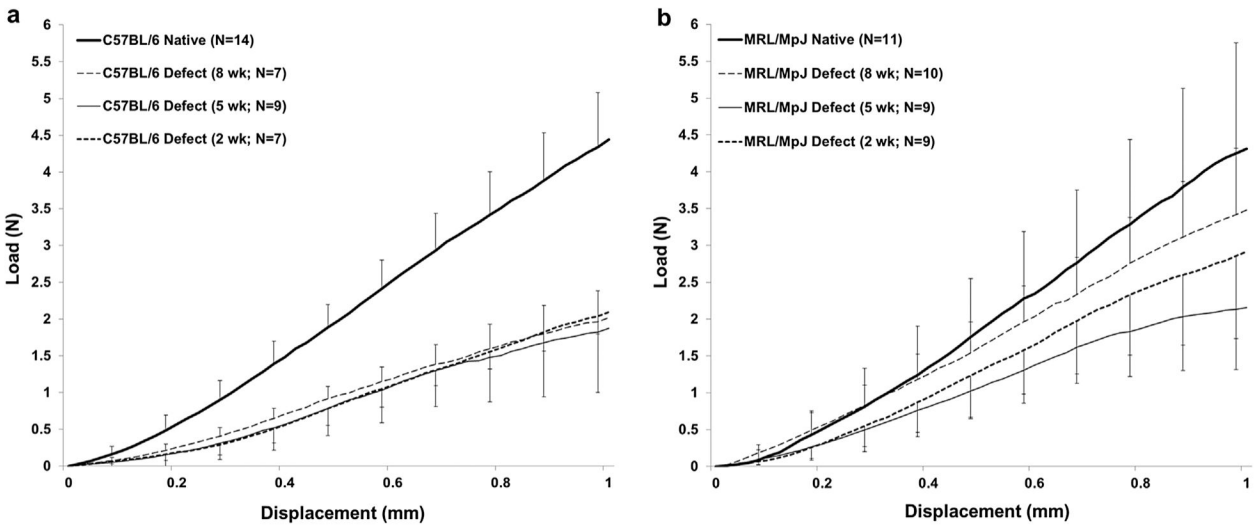

Figure 2.

Average load-displacement failure curves for repair tissue at 2, 5, and 8 weeks for the C57BL/6 and MRL/MpJ strains. (a) The C57BL/6 healing tissue was significantly inferior to native tissue with respect to structural properties at all time points following injury ($p < 0.05$). (b) The MRL/MpJ healing tissue was significantly less than native tissue at 2 and 5 weeks; however, by 8 weeks, the MRL/MpJ reached native values with respect to ultimate load (3.48 ± 0.92 N vs. 4.31 ± 1.53 N, $p > 0.05$). Error bars indicated SD.

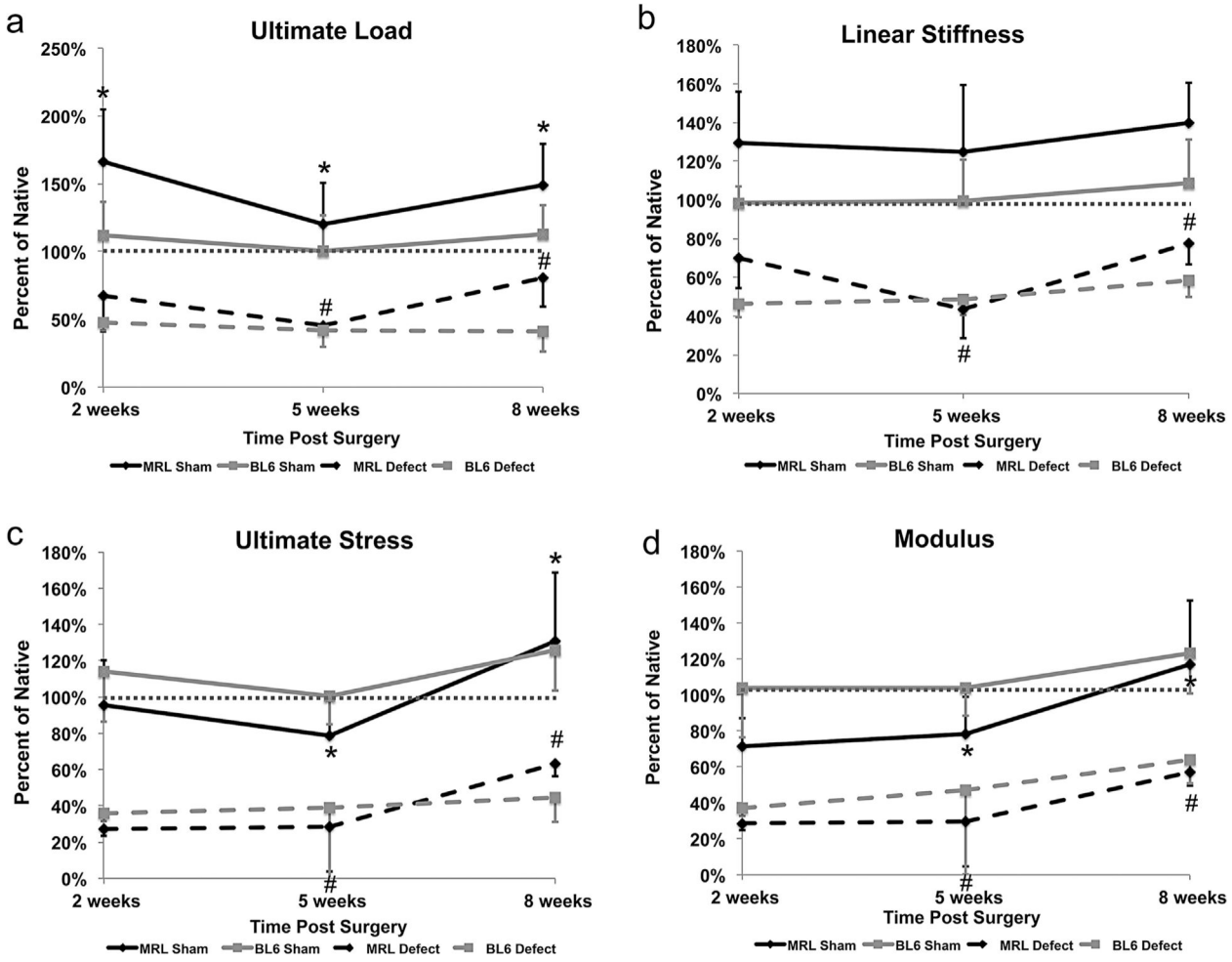

Figure 3.

Structural and material properties of defect and sham tendon tissues plotted as a percent of native for (a) ultimate load, (b) linear stiffness, (c) ultimate stress, and (d) modulus. The MRL/MpJ repair tissue exhibited improved structural and material properties between 5 and 8 weeks post surgery, while the C57BL/6 failed to display significant improvements beyond the 2-week time point. Statistical tests were performed on raw data. Error bars indicate SD (*significantly different with respect to time for MRL/MpJ sham tissue ($p < 0.05$); #significantly different with respect to time for MRL/MpJ defect tissue ($p < 0.05$).

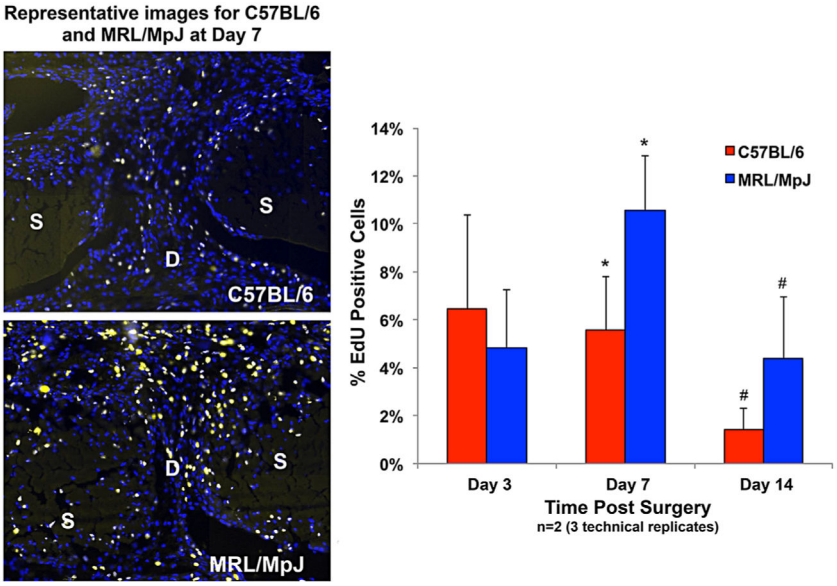

Figure 4.

The MRL/MpJ shows increased cellular proliferation compared to C57BL/6 ($p < 0.05$) at 7 and 14 days in the tendon healing region as measured by the number of EdU positive cells normalized to total cell number. The images are representative of the defect region for C57BL/6 and MRL/MpJ 7 days following injury (DAPI-Blue, EdU-Yellow). S: Strut, D: Defect. Error bars indicate SD.

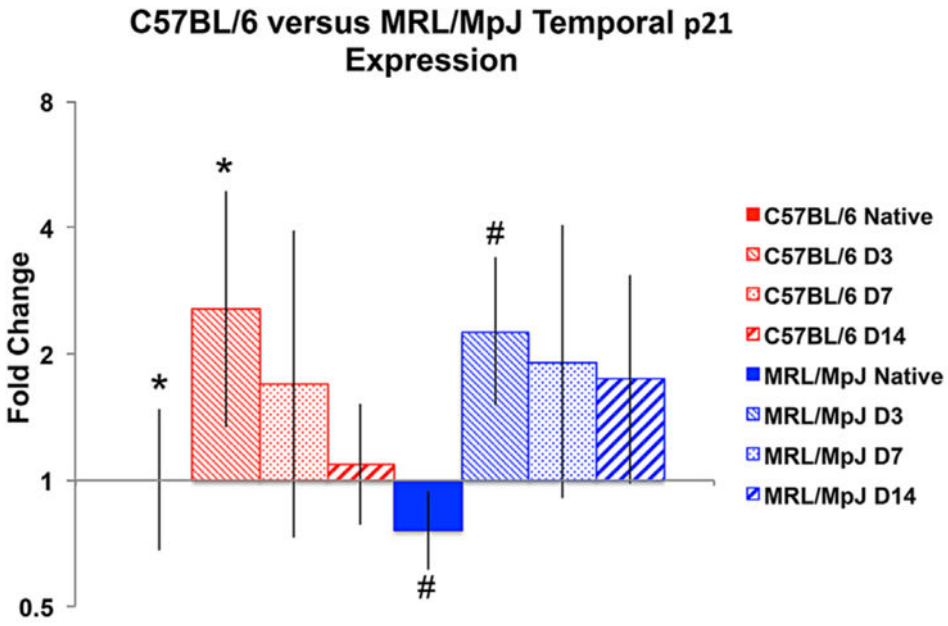

Figure 5.

The C57BL/6 and MRL/MpJ strains show similar temporal expression of the cell cycle regulator, p21, following tendon injury. At day 3, both the C57BL/6 and MRL/MpJ showed significantly increased expression of p21 compared to respective native controls ($p < 0.05$).

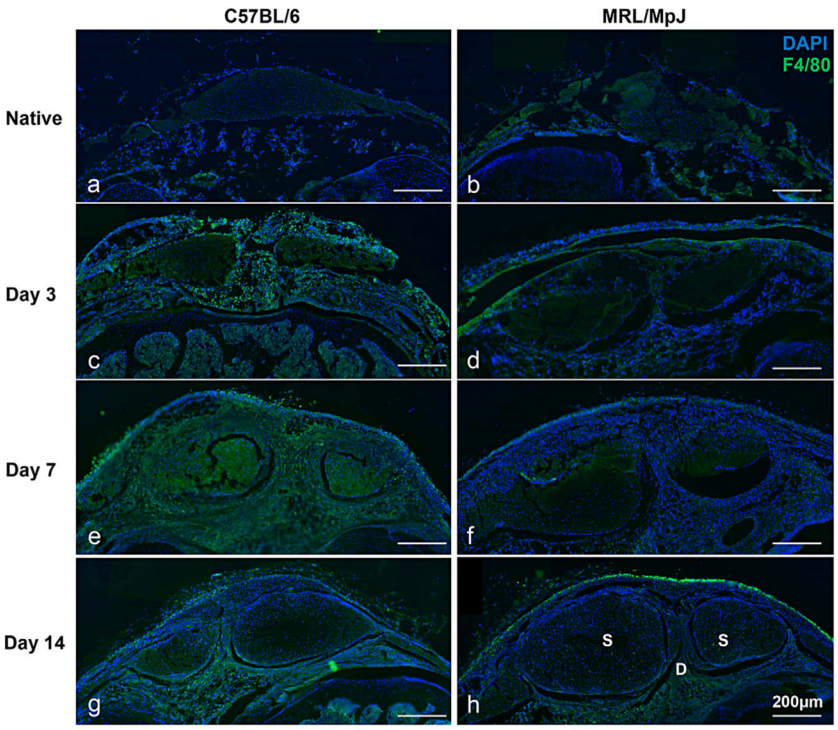

Figure 6.

The MRL/MpJ strain shows a decreased immune response following tendon injury. F4/80 staining showed no differences between the C56BL/6 and MRL/MpJ native tissue (a,b); however by 3 days, infiltrating macrophages are present in the paratenon, struts, fat pad, and healing region of the C57BL/6 (c) while the MRL/MpJ response is predominant in the paratenon only (d). By 7 days, macrophage infiltration peaks in the C57BL/6, but remains reduced in the MRL/ MpJ (e, f). At day 14, the response has reduced in both strains, concentrated to the paratenon and fat pad (g, h). In image h, S-Strut and D-Defect.

Table 1

Experimental Design

Treatment	0	3	7	14	35	56
DEFECT						
C57BL/6						
Histology/IHC		2	2	2		
qPCR		9*	9*	9*		
Biomechanics				7	9	7
MRL/MpJ						
Histology/IHC		2	2	2		
qPCR		9*	9*	9*		
Biomechanics				8	10	10
SHAM						
C57BL/6						
Histology/IHC		2	2	2		
Biomechanics				7	9	7
MRL/MpJ						
Histology/IHC		2	2	2		
Biomechanics				8	10	10
NATIVE						
C57BL/6						
Histology/IHC	2					
qPCR	9*					
Biomechanics	14					
MRL/MpJ						
Histology/IHC	2					
qPCR	9*					
Biomechanics	11					

The asterix indicates that tissue was collected from 9 animals, but the resulting mRNA was pooled to have a final of 3 independent samples each with mRNA from 3 animals.

Table 2

Gene Symbol and Gene Expression Assay ID Numbers

Name	Symbol	Gene Expression Assay ID
Eukaryotic 18S rRNA	18s	Hs99999901_s1
Collagen Type I, alpha 1 chain	Col1a1	Mm00801666_g1
Collagen Type III, alpha 1 chain	Col3a1	Mm01254476_m1
Decorin	Dcn	Mm00514535_m1
Fibromodulin	Fmod	Mm00491215_m1
Tenascin-C	TnC	Mm00495662_m1
Tenomodulin	Tnmd	Mm00491594_m1
Scleraxis	Scx	Mm01205675_m1
Mohawk Homeobox	Mkx	Mm00617017_m1
Early Growth Response-1	Egr1	Mm00656724_m1
Cyclin-Dependent Kinase Inhibitor 1A	p21	Mm04205640_g1
Myelocytomatosis Oncogene	Myc	Mm00487804_m1
Interferon Gamma	Ifng	Mm01168134_m1
POU Domain, Class 5, Transcription Factor 1	Pou5f1	Mm03053917_g1
Homeobox A13	Hoxa13	Mm00433967_m1

Table 3

Mechanical Properties for C57BL/6 and MRL/MpJ Native, Defect, and Sham (mean ± SD)

	Cross-Sectional Area (mm^2)	Ultimate Load (N)	Linear Stiffness (N/mm)	Max Stress (MPa)	Modulus (MPa)
C57BL/6					
Native PT ($n = 14$)	0.28 ± 0.04	4.44 ± 0.75	9.76 ± 1.30	16.20 ± 2.72	105.30 ± 20.11
2-week Defect ($n = 8$)	0.38 ± 0.07	2.10 ± 0.25[a]	4.50 ± 0.66[a]	5.80 ± 0.72[a]	39.03 ± 6.45[a]
2-week Sham ($n = 8$)	0.28 ± 0.02	4.98 ± 1.08	9.61 ± 0.83	18.48 ± 7.57	109.57 ± 30.11
5-week Defect ($n = 9$)	0.31 ± 0.06	1.87 ± 0.55[a]	4.74 ± 0.79[a]	6.31 ± 2.19[a]	49.53 ± 15.12[a]
5-week Sham ($n = 9$)	0.28 ± 0.05	4.45 ± 1.17	9.73 ± 2.08	16.23 ± 4.49	109.11 ± 28.12
8-week Defect ($n = 7$)	0.25 ± 0.03	1.82 ± 0.66[a]	5.72 ± 0.85[a]	7.24 ± 2.47[a]	67.63 ± 11.62[a]
8-week Sham ($n = 7$)	0.25 ± 0.03	4.99 ± 0.97	10.61 ± 2.20	20.37 ± 3.64	129.45 ± 29.26
MRL/MpJ					
Native PT ($n = 11$)	0.25 ± 0.03	4.31 ± 1.53	9.31 ± 1.99	17.85 ± 6.72	130.96 ± 39.99
2-week Defect ($n = 8$)	0.54 ± 0.12[a]	2.91 ± 1.15[a]	6.50 ± 1.43[a]	5.33 ± 1.64[a]	39.37 ± 7.27[a]
2-week Sham ($n = 8$)	0.42 ± 0.07	7.18 ± 1.65	12.06 ± 2.47	17.01 ± 4.44	93.20 ± 20.92
5-week Defect ($n = 10$)	0.39 ± 0.07[a]	1.96 ± 0.29[a]	4.06 ± 1.40[a]	5.12 ± 1.31[a]	38.44 ± 12.87[a]
5-week Sham ($n = 10$)	0.38 ± 0.05	5.11 ± 1.25	11.06 ± 3.47	13.82 ± 3.29	98.50 ± 27.74
8-week Defect ($n = 10$)	0.31 ± 0.08	3.48 ± 0.92[b]	7.21 ± 1.00[a]	11.33 ± 3.73[a]	74.49 ± 20.67[a]
8-week Sham ($n = 10$)	0.29 ± 0.07	6.42 ± 1.30	13.02 ± 1.91	23.39 ± 6.77	153.00 ± 46.73

[a] Significantly different from respective native ($p < 0.01$).

[b] Significantly different from C57BL/6 at corresponding time point ($p < 0.01$).

Table 4

Delta Ct values for genes of interest measured in C57BL/6 and MRL/MpJ native and defect tissue

	Col1a1	Col3a1	Dcn	Egr1	Fmod	Mkx	Scx	Tnc	Tnmd	Myc	p21
C57BL/6											
Native	8.4 ± 0.6	11.4 ± 1.1	10.4 ± 0.4	19.2 ± 1.0	12.2 ± 0.1	17.8 ± 0.4	16.1 ± 0.1	15.7 ± 1.9	14.4 ± 0.6	18.8 ± 0.5	17.5 ± 0.6
D3 Defect	8.5 ± 0.1	10.1 ± 0.1	12.7 ± 0.3	18.9 ± 0.6	17.8 ± 0.9[a]	21.7 ± 0.9	17.5 ± 0.8	14.3 ± 0.2	18.3 ± 0.9	17.2 ± 0.3	16.1 ± 0.4
D7 Defect	6.5 ± 0.5	8.4 ± 0.5[a]	11.4 ± 0.8	19.2 ± 1.0	14.3 ± 1.2	19.0 ± 1.5	15.5 ± 0.7	13.6 ± 0.7	14.4 ± 1.2	17.5 ± 0.8	16.7 ± 0.6
D14 Defect	7.4 ± 1.5	9.9 ± 0.8	11.3 ± 0.5	19.1 ± 0.8	13.4 ± 1.4	19.1 ± 0.9	16.2 ± 1.5	15.3 ± 1.6	13.8 ± 1.7	19.6 ± 1.2	17.3 ± 0.6
MRL/MpJ											
Native	9.7 ± 0.6	12.0 ± 0.8	11.3 ± 0.5	20.1 ± 0.1	13.4 ± 0.7	18.6 ± 0.7	16.3 ± 0.4	17.4 ± 1.5	14.8 ± 0.9	19.2 ± 0.2	17.9 ± 0.3
D3 Defect	8.6 ± 0.2	10.0 ± 0.3	13.8 ± 0.5	19.8 ± 1.2	18.7 ± 1.8	21.8 ± 0.9	18.1 ± 1.0	13.7 ± 0.4	19.1 ± 1.8	17.1 ± 0.4	16.3 ± 0.1
D7 Defect	7.0 ± 0.7[a]	8.3 ± 0.8[a]	11.9 ± 1.2	18.9 ± 0.9	14.7 ± 1.1	19.2 ± 1.3	16.1 ± 0.8	13.3 ± 0.7[a]	14.1 ± 1.0	17.7 ± 0.7	16.5 ± 0.9
D14 Defect	7.4 ± 0.5	9.0 ± 0.8	11.9 ± 0.9	18.6 ± 1.2	13.4 ± 0.5	18.9 ± 0.7	16.4 ± 0.5	14.6 ± 0.6	13.1 ± 0.7	18.7 ± 1.0	16.7 ± 0.8

[a]Significantly different than respective native control ($p < 0.01$).